

PREPARATION AND CHARACTERIZATION OF POLYMER/CDS NANOSTRUCTURED PHOTOLUMINESCENT FILMS

M. Iovu¹, I. Tighineanu², I. Culeac¹, S. Robu³, Iu. Nistor¹, G. Dragalina³,
M. Enachi⁴, P. Petrenko¹, V. Verlan¹

¹*Institute of Applied Physics, Nr. 5 Academiei Str., Chisinau MD 2028, Republic of Moldova*

²*Institute of Electronic Engineering & Nanotechnologies, Nr 3/3 Academiei Str.,
Chisinau MD 2028, Republic of Moldova*

³*Moldova State University, Nr. 60 Mateevici Str., Chisinau MD 2009, Republic of Moldova*

⁴*Technical University of Moldova, Nr. 168 Stefan cel Mare Str.,
Chisinau MD 2012, Republic of Moldova*

Abstract: We present experimental results on polymer-based nanocomposites based on styrene with butyl methacrylate (SBMA) (1:1), isothiocyanato-chalcone (ITCC) and inorganic semiconductor CdS. Thin film composite samples have been characterized by UV-Vis absorption and photoluminescent (PL) spectroscopy, X-ray diffraction, as well as by atomic-force microscopy (AFM). The surface of nanocomposites SBMA+10%ITCC+10%CdS films exhibits a quasi-ordered structure with conic-shaped elements 25-50 nm high, almost regularly distributed on the surface of the films. The average CdS particles size estimated from the X-ray diffraction pattern correlates with the corresponding value obtained from the UV-Vis absorption spectrum, and was found to be in the range 9-17 nm. The PL emission spectra have been registered at room temperature under the excitation of laser beam 337 nm or 405 nm, both in SBMA/CdS samples as well as in NC samples made of SBMA/ITCC/CdS.

1. Introduction

Nanocomposite materials have attracted attention in both fundamental studies as well as technical applications. This is basically due to the possibility of tuning of their physical and chemical parameters through varying the size of nanoparticles.¹⁻³ The polymers are widely used in the technology of preparation of nanocomposite materials in the quality of matrix that serves for assembling the nanoparticles into clusters and for avoiding the agglomeration, as a matrix in self-assembling nanomaterials that induce ordering and anisotropic orientation, as well as acting as a functional element.^{4,5} The polymer-inorganic nanocomposite materials possess important advantages, among them, mechanical strength, a simple technology and low cost.^{1,3} They are characterized by ease of processing and control of the shape of materials, and can be prepared by different methods of spin-coating, casting, extrusion, etc.^{4,6-8}

Nanocomposite materials based on inorganic semiconductors incorporated in polymeric or in glass matrix exhibit advanced optical properties and stability during the long time exploitation in comparison to purely polymer-made devices.⁷⁻¹⁰ Because of the quantum confinement of electrons and photons inorganic semiconductor nanoparticles used in the nanocomposites exhibit physical and chemical properties which are different from the properties of corresponding bulk materials, and this can be used for fine tuning of the properties of nanocomposite structures.^{5,7,11} Among various inorganic nanoparticles CdS have received great attention because of their attractive properties and potential for application in photonics and optoelectronics.¹²⁻¹⁵ Further investigation of the polymer-based nanocomposites are equally important for understanding the mechanism of transport and

photoluminescence in these materials, developing of materials with advanced characteristics, as well as for possible minimizing the toxicity of Cd-based materials. In the present work we report preparation and characterization of polymer-inorganic nanocomposite thin films based on styrene with butylmethacrylate (SBMA) (1:1), isothiocyanato-chalcone (ITCC) and inorganic semiconductor CdS.

2. Experimental

The photoluminescent nanocomposites based on styrene with butylmethacrylate (SBMA) (1:1), isothiocyanato-chalcone (ITCC) and inorganic semiconductor CdS were prepared by simple chemical method¹⁶⁻¹⁸ using organic solvents instead of water. The cyanato-chalcone derivate was used as mechanical additive, as well as for chemical bonding in the polymer, which makes the final composite more stable. For preparation of the nanodimensional composites we have used an aromatic chalcone with organic polymer – isothiocyanato-chalcone. The polymer made of styrene with butylmethacrylate (SBMA) (1:1) exhibits the following physico-chemical characteristics: Viscosity $[\eta] = 0.26$ dl/g; Vitrification temperature $T_v = 63-64^\circ\text{C}$; Flow temperature $T_f = 89-90^\circ\text{C}$. Preparation of the nanocomposites was described elsewhere.¹⁹ The composite layers were obtained on clean glass substrates or on SnO₂-covered glass substrates for measuring of photoluminescence and electroluminescence. The thickness of the thin film layers was in the range 5-15 μm . Nanocomposite thin films were characterized by measuring UV-Vis transmission and PL spectra, by atomic force microscopy and X-ray diffraction. The measurements of atomic force microscopy (AFM) were performed using a Nanoscope IIIa (digital

Instruments, Santa Barbara, CA) in contact mode. Optical transmission spectra of the samples were registered in the range 400–800 nm on a Specord UV-Vis spectrophotometer, to determine the energy band gap. PL spectra of nanocomposite thin films were measured under excitation of a laser beam 337 or 405 nm using a MDR-23 monochromator and a photomultiplier detector. X-ray diffraction patterns were recorded using a DRON-UM diffractometer (Fe K_{α} - radiation, $\lambda = 1.93604 \text{ \AA}$, θ - 2θ - method).

3. Discussion

Examination of prepared thin films suggests that they contain clusters of CdS of different sizes. It was established that the SBMA/ITCC/CdS composite thin films exhibits a strong tendency to self-organization. This clearly can be seen on nanocomposite thin films SBMA+10%ITCC+10%CdS deposited on SnO₂-covered glass substrate (Fig. 1).

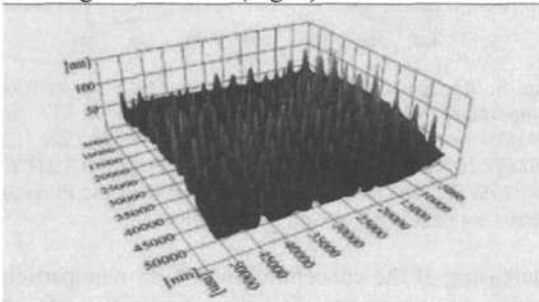


Fig. 1. AFM 3D image of surface of SBMA+10%ITCC+10%CdS thin film deposited on glass substrate covered with SnO₂.

In this case the surface morphology can be described as quasi-ordered structure with conic-shaped elements almost regularly distributed on the surface of the films. The average height of conic-shaped elements varies in the range 25-50 nm (Fig. 1). The distance between these domains is about 4 μm , while the average diameter of the domain is around 1.5 μm . A similar situation was observed with thin films of other compositions, but with less ordered structure.

Fig. 2 illustrates the results for X-ray diffraction (XRD) measurements for the nanocomposite thin-film samples SBMA+10%ITCC+10%CdS. The XRD pattern provides information on the crystalline phase of embedded nanoparticles, as well as on the particle size. The XRD pattern of the composite SBMA+10%ITCC+10%CdS deposited on SnO₂-covered glass consists of the weak reflections of CdS, the pronounced reflections of the SnO₂ thin film and some reflections related with a presence of the ITCC and glass substrate. The polycrystalline CdS has an orthorhombic syngony,^{20,21} of the space group $Pnnn$, $a = 14.315 \text{ \AA}$, $b = 14.074 \text{ \AA}$, $c = 14.568 \text{ \AA}$.

The diffraction peaks were observed on the XRD pattern of the sample SBMA+10%ITCC+10%CdS (Fig. 2(b)) corresponding to the orthorhombic phase of CdS nanoparticles.^{20,21} The size D of the CdS particles was determined by the width of the most intense peak by the well-known Scherer relation.^{22,23}

$$D = k\lambda / \beta \cos \theta,$$

where k is the constant equal to 1 for orthorhombic crystal²³, λ is the X-ray radiation wavelength equal to 1.93604 \AA ; β is the full width at half maximum (FWHM) of the XRD selected diffraction peak on the 2θ scale, and θ is the diffraction angle. The particle size calculated from XRD line width is 12-14 nm.

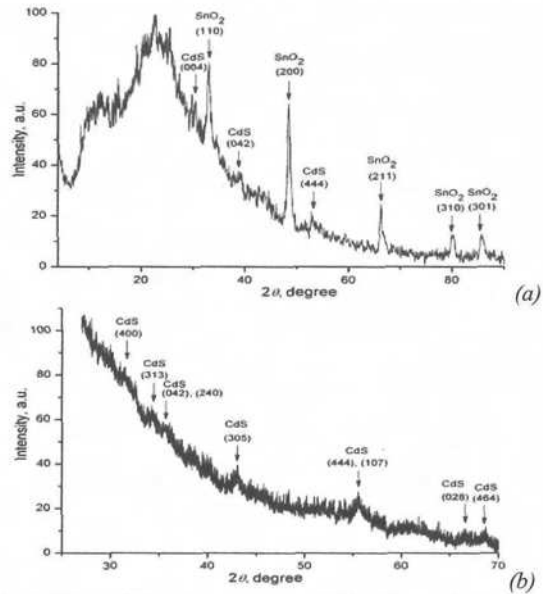


Fig. 2. X-ray diffraction patterns of thin films: (a) SBMA + 10%ITCC + 10%CdS deposited on SnO₂-covered glass; (b) SBMA + 10%ITCC + 10%CdS deposited on glass.

The UV-Vis absorption spectra of nanocomposite thin-film samples deposited on glass substrates are represented in Fig. 3 and 4. The fundamental absorption, which corresponds to electron excitation from the valance to conduction bands, can be used to determine the value of the optical band gap.^{24,25}

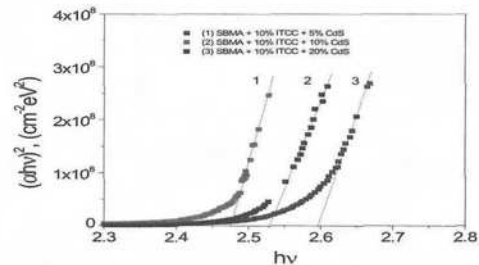


Fig. 3. The dependence of $(\alpha h\nu)^2$ versus $h\nu$ for different compositions of the nanocomposite thin films for determination of the band edge E_g .

The optical band gap E_g has been evaluated using the relation:²⁴⁻²⁶

$$(\alpha h\nu)^{1/n} = A(h\nu - E_g),$$

where α is the absorption coefficient, $h\nu$ is the incident photon energy, A is a constant, and the exponent n depends on the type of transition. As CdS is a direct band gap material, $n = 1/2$ for the allowed transition.¹³ The band gap has been calculated by extrapolating the linear region of the plot $(\alpha h\nu)^2$ vs $h\nu$ on the energy axis, as shown in Fig. 3. The band gaps for the samples SBMA/ITCC/CdS with the concentration of 5, 10, and 20 % CdS are obtained as

2.47, 2.52, and 2.57 eV, respectively. These values are higher than E_g of the bulk CdS (2.42 eV at 300 K^{8,13}) which is indicative of a blue shift of the absorption edge.

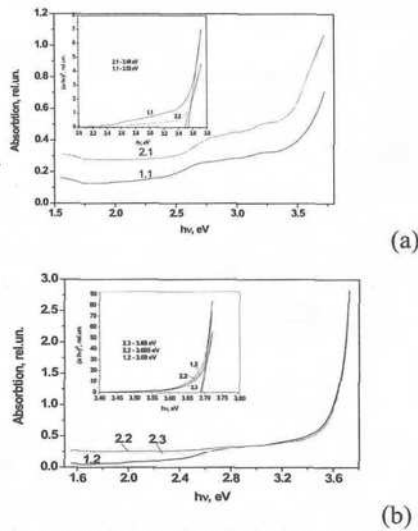


Fig. 4. The dependence of optical absorption of photon energy for composite samples SBMA+20%CdS (1.1; 1.2) and SBMA+40%CdS (2.1, 2.2, 2.3).

The XRD spectra in Fig. 2(b) suggest that the CdS nanoparticles are in a polycrystalline form, i.e., they consist of a large number of small crystallites. The increase of the band gap may be attributed to the quantum size effect of these small crystallites, although the calculated diameter of the nanocrystals are larger than the excitonic Bohr radius ~ 3 nm of CdS.^{2,13} One can be seen (Fig. 3) that the band gap varies from 2.47 to 2.58 eV, which can be explained by the decrease of the size CdS crystallite as the concentration of CdS increases. The UV-Vis absorption spectrum of the nanocomposite thin films in Fig. 3 indicates on a blue shift in the absorption edge when the concentration of the CdS increases from 5 to 20 %. This shift, along to registered X-ray diffraction patterns suggest that the CdS nanoparticles are quantum-confined. Consequently, from the shift of the absorption edge the size of the CdS nanoparticles are calculated based on the effective mass approximation approach:²⁴⁻²⁷

$$E_{gn} = \sqrt{E_{gb} + \frac{2\hbar^2 E_{gb} (\pi/R)^2}{m^*}},$$

where E_{gn} is the band gap of the nanocomposite, E_{gb} is the band gap of the bulk CdS, m^* is the effective electron mass ($= 0.2$ times the mass of a free electron), and $\hbar = h/2\pi$ (h is the Planck constant). If we take for the bulk CdS $E_g = 2.42$ eV^{8,27}, then the calculated diameter of the CdS particles obtained from the band gap shift (Fig. 3) are as listed in Table 1. Consequently, the CdS particle size for the SBMA+10%ITCC+10%CdS is found to be 12 nm compared to the average size 13 nm obtained from the XRD measurements.

PL spectra of polymeric nanocomposites were investigated at room temperature in the range 360-800 nm under excitation with laser beam 337 nm or

405 nm. Fig. 5 represents the PL spectra of nanocomposites SBMA/ITCC/CdS with different concentrations of CdS measured at room temperature.

Table 1.

Band gap energy and the diameter of the CdS nanoparticles as calculated from the plot $(\hbar\nu)^2$ vs. $\hbar\nu$ in Fig. 3.

Nanocomposite	E_{gn} , (eV)	D, (nm)
SBMA+ITCC+5%CdS	2.47	17.19
SBMA+10%ITCC+10%CdS	2.52	12.09
SBMA+10%ITCC+20%CdS	2.58	9.5

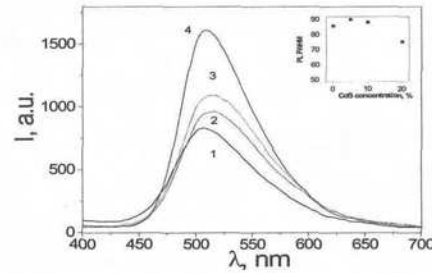


Fig. 5. PL spectra for the nanocomposite films at room temperature when excited with UV light $\lambda=337$ nm: SBMA+10%ITCC (1); SBMA+10%ITCC+5%CdS (2); SBMA+10%ITCC+10%CdS; (3); SBMA+10%ITCC+20%CdS (4). The insert shows the FWHM of the PL peaks versus concentration of CdS nanoparticles.

Increasing of the concentration of CdS nanoparticles leads to increase in the intensity of the photoluminescence and shifts the maximum of the photoluminescence peak in the high energy region. The PL emission peaks of the nanocomposites SBMA/ITCC/CdS are found to be located around 2.45, 2.40, 2.41 and 2.44 eV respectively (curves 1, 2, 3, 4 in Fig. 5). The optical band gap of the nanocomposites with the content 5, 10, and 20% CdS determined from the extrapolation of the plot $(\hbar\nu)^2$ vs. $\hbar\nu$ in Fig. 3 corresponds to 2.47, 2.52, and 2.57 eV respectively. This indicates that the luminescence peaks are Stokes-shifted from their band gap energy. The full width at half maximum (FWHM) of the PL peak slightly decreases with increasing the concentration of CdS nanoparticles in the composite material (Fig. 5). FWHM value slightly varies in the range 74-92 nm. This suggests the size distribution of the nanoparticles around the mean diameter value. As far as emission energies of the nanocomposite samples are lower than the corresponding band gap energies, one may suppose that the luminescence may originate from the radiative recombination involving donors and acceptor centers.¹³

Nanocomposite samples SBMA+CdS exhibit a strong luminescent signal in the range 350-600 nm (edge maximum, A), with the position of PL maximums varying in dependence of the dimensions of the CdS nanoparticles in polymer matrix. In addition in the 550-750 nm range one can observe several weaker maximums at ~ 600 nm (B1) and ~ 650 nm (B2). The PL maximums A can be attributed to direct transitions from the conduction band to valence, while B1 and B2 bands - to the transitions between donor levels to the valence band of CdS. While varying the excitation wavelength one can observe the redistribution of PL intensity between A and B.

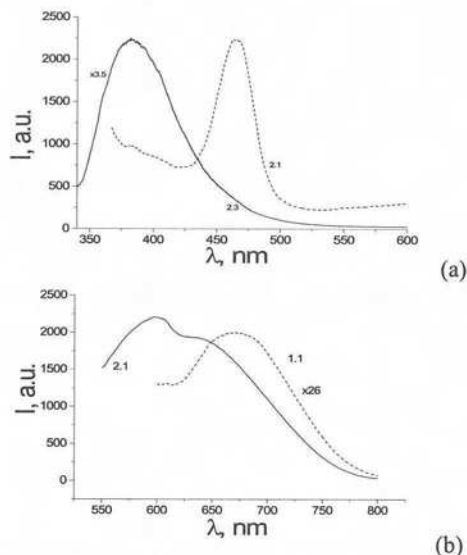


Fig. 6. PL spectra of nanocomposite samples at room temperature: SBMA+20%CdS (1.1); SBMA+40%CdS (2.1, 2.3). The excitation light: $\lambda_{exc} = 337$ nm (a); 405 nm (b).

4. Summary

Polymer-based nanocomposites made of styrene with butyl methacrylate, isothiocyanato-chalcone and inorganic semiconductor CdS have been investigated. The concentration of CdS semiconductor was varied in the range 0-20 %. Examination of the thin film surface of SBMA+10%ITCC+10%CdS films by AFM microscope showed that the surface of these composites can be described as quasi-ordered structure with conic-shaped elements, 25-50 nm high, almost regularly distributed on the surface of the films. The average CdS particle size estimated from the X-ray diffraction correlates with those obtained from the UV-Vis absorption spectrum and were found to be in the range 9-17 nm. The nanocomposite samples exhibit a strong luminescent in the visible range 350-600 nm.

Acknowledgment: The work was supported by the Institutional Project of the Academy of Science of Moldova Nr. 11.817.05.03A as well as by the Project within the State Program Nr. 11.836.05.04A.

References

1. D. R. Paul and L. M. Robeson, *Polymer* 49, 3187 (2008).
2. Y. Wang and N. Herron, *J. Phys. Chem.* 95, 525 (1991).
3. S. Li, M. M. Lin, M. S. Toprak, D. K. Kim, and M. Muhammed, *Nano Reviews* 1, 5214 (2010).
4. R. Shenhar, and T. B. Norsten, *Adv. Mater.* 17, 657 (2005).
5. D. Y. Godovsky, Device applications of polymer-nanocomposites. *Advances in Polymer Sciences*, Springer-Verlag, Berlin Heidelberg (2000), Vol. 153.
6. M. Ando, Y. Kanemitsu, T. Kushida, K. Matsuda, T. Saiki, and C. W. White, *Appl. Phys. Lett.* 79, 539 (2001).

7. J. R. Lakowicz, I. Gryczynski, Z. Gryczynski, and C. J. Murphy, *J. Phys. Chem. B* 103, 7613 (1999).
8. H. Yoon, Y.-M. Rhym, and S. E. Shim, *Colloid Polym. Sciences* 289, 1185 (2011).
9. N. Sounderya and Y. Zhang, *Recent Patents on Biomedical Engineering* 1, 34 (2008).
10. P. Chouksey, M. Tiwari, and B. P. Chandra, *Intern. J. Advanced Engineering & Applications* 106 (2011).
11. M.-J. Almendara-Parra, A. Alonso-Mateos, S. S. Paradinas, J. F. Boyero-Benito, E. Rodriguez-Fernandez, and J. J. Criado-Talavera, *Journal of Fluorescence* 22, 59 (2012).
12. X. Chen, Z. T. Yu, J. S. Chen, and B. Yang, *Mater. Lett.* 58, 384 (2004).
13. S. P. Mondal, H. Mullick, T. Lavanya, A. Dhar, S. K. Ray, and S. K. Lahiri, *J. Appl. Phys.* 102, 064305 (2007).
14. M. Z. Rong, M. Q. Zhang, H. C. Liang, and H. M. Zeng, *Appl. Surf. Sci.* 228, 176 (2004).
15. R. R. Prabhu and M. Abdul Khadar, *PRAMANA Journal of Physics* 65, 801 (2005).
16. M. Caraman, S. Robu, P. Gasin, and I. Lazer, *Proc. SPIE* 7297, 729717
17. N. Barba, A. Popusoi, C. Lozan-Tirus, J. Roy, D. Piorier, A. Gulea, Aromatic isothiocyanato-propenones and thiourea derivatives. Synthesis and biological properties. *1-er Colloque Franco-Roumain de Chimie Medicale*, Romania (2010), p. 52.
18. A. Popusoi, N. Barba, G. Dragalina, E. Cuculescu, M. Caraman, and S. Robu, Nanocompozite polimerice fotoluminescente din derivati ai chalconelor aromatice. *PRIOCHIM*, Sinaia, Romania, October (2009), p. 44.
19. M. Iovu, I. Tiginyanu, I. Culeac, S. Robu, Iu. Nistor, G. Dragalina, M. Enachi, and P. Petrenko, Nanostructured Polymer/CdS Photoluminescent Thin Films, *Journal of Nanoelectronics and Optoelectronics* Vol. 7, 1-5, 2013
20. Joint Committee on Powder Diffraction-International Centre for Diffraction Data, (JCPDS-ICDD), 1997, 47-1179.
21. Joint Committee on Powder Diffraction-International Centre for Diffraction Data, (JCPDS-ICDD), 1997, 46-1088.
22. Z. R. Khan, *J. Mater. Sci.* 46, 5412 (2011).
23. M. Pattaby, B. S. Amma, and K. Manzoor, *Mater. Res. Bull.* 42, 828 (2007).
24. M. Z. Rong, M. Q. Zhang, H. C. Liang, and H. M. Zeng, *Appl. Surf. Sci.* 228, 176 (2004).
25. Y. Wang and W. Mahler, *Optical Communications* 61, 233 (1987).
26. Y. Wang, A. Suna, W. Mahler, and R. Kasowski, *The Journal of Chemical Physics* 87, 7315 (1987).
27. F. A. Kasim, M. A. Mahdi, J. J. Hassan, S. K. J. Al-Ani, and S. J. Kasim, *International Journal of Nanoelectronics and Materials* 5, 57 (2012).